Optical refractive index and static permittivity of mixed Zr–Si oxide thin films prepared by ion beam induced CVD

F.J. Ferrer [a,*], F. Frutos [b], J. García-López [a], A.R. González-Elipe [c], F. Yubero [c]

[a] Centro Nacional de Aceleradores, Av. Thomas A. Edison, 7, 41092 Sevilla, Spain
[b] E.T.S. de Ingeniería Informática, Avda. Reina Mercedes, s/n, 41012 Sevilla, Spain
[c] Insituto de Ciencia de Materiales de Sevilla, c/ Americo vespucio, no. 49, 41092 Sevilla, Spain

1. Introduction

Mixed Zr–Si oxide thin films are very interesting materials because of their use as optical coatings of tailored refractive index [1] and also because they are candidates to replace SiO_2 as gate oxide in MOS devices [2] due to their high permittivity and electrical insulation properties. For these applications, obtaining flat, compact and amorphous films at room temperature is specially indicated.

Permittivity is a physical quantity that is determined by the ability of a material to polarize in response to an external field. The permittivity of a material is usually referred to that of vacuum, as a relative permittivity (also called dielectric constant). In general, the relative permittivity or dielectric constant is a function of the frequency of the electromagnetic field used in its evaluation. Within the microelectronic scientific community the dielectric constant, calculated from the C–V measurements at 0.1–1 MHz is usually called permittivity or static dielectric constant and takes the symbol k. On the other hand, the dielectric constant obtained from optical methods as ellipsometry, reflection or transmission spectroscopies in the visible range (frequencies 10^{14}–10^{15} Hz) is usually presented as the refractive index n evaluated at a given wavelength (the refractive index is equal to the square root of the dielectric constant for non-absorbing materials). In the former case, ionic, dipolar and electronic relaxations are responsible for the variation of the permittivity, while in the latter case, changes in the electronic relaxation processes show up in the optical dielectric constant of a given material.

The study of static permittivity and optical dielectric constants of zirconium silicates thin films have been attempted before theoretically [3,4]. A general good agreement has been found between theory and experiments regarding the relation between optical dielectric constants (and refractive index) and stoichiometry in Zr–Si–O mixed oxides thin films. However, there is controversy on the relation between the static permittivity and the Zr content in the silicates [3,4].

In this paper we report on the optical refractive index and static permittivity of mixed $Zr_xSi_{1-x}O_2$ oxide films produced by

* Corresponding author. Tel.: +34 954 460 553; fax: +34 954 460 145.
E-mail address: fjferrer@us.es (F.J. Ferrer).

means of ion beam induced chemical vapour deposition (IBICVD) [5,6]. It is known that the use of ion beams to assist the deposition of this kind of films leads to the formation of compact and smooth thin films [5]. This method has been previously used to produce the single SiO_2 [10,11] and ZrO_2 [12] oxides and other mixed oxide as titanium aluminates [7,8] or titanium silicates [9].

2. Experimental

Mixed oxides $Zr_xSi_{1-x}O_2$ ($0<x<1$) thin films have been prepared at room temperature by decomposition of triethoxysilane $(CH_3CH_2O)_3SiH$ (TrEOS) and zirconium tetra-tert-butoxide $Zr[OC(CH_3)_3]_4$ (ZTB) volatile precursors induced by ion bombardment. The choice of these precursors for this study is justified by the fact that ZTB and TrEOS are extensively used in the literature to grow pure silicon oxide, zirconium oxide and zirconium silicates due to their high vapour pressure and general low temperature for synthesis of the mentioned oxides [9,13–15]. The precursors were dosed into the reactor (base pressure $\sim 1\times10^{-4}$ Pa) using leak valves with partial pressures in the range between 5×10^{-4} and 2×10^{-3} Pa. A broad beam ion source (HFQ 1303-3), excited by a RF discharge of Ar/O_2 mixtures (80% Ar and 20% O_2 regarding relative partial pressures) at about 1×10^{-1} Pa, was used to supply bombarding ions with 400 eV. The ionization efficiency of O_2 gas in a RF plasma is less than that of a mixture of Ar/O_2 gasses, so it is expected that the relative amount of bombarding Ar^+/O_2^+ ion ratio is enhanced with respect to the Ar/O_2 partial pressure ratio in the reactor. The ion beam current density measured at the sample position was about 5–10 μA/cm^2. In these conditions, the deposition rate was ~1 nm/min. Thin films with thicknesses in the range of 50 to 400 nm were produced. More experimental details regarding the deposition technique can be found elsewhere [5,6].

Polished Si(100) wafers were used as substrates. For electrical measurements the Si wafers were doped and had an electrical conductivity between 1 and 5 Ωcm. For Infrared analysis the Si was intrinsic in order to avoid absorption in the infrared region.

Surface composition and chemical analysis of the thin films was performed by means of X-ray photoelectron spectroscopy (XPS) using a PHOIBOS100 electron spectrometer.

Thin film composition was obtained by combined Ion Beam Analysis techniques using the 3 MV tandem accelerator of National Centre for Accelerators (Seville, Spain) [16]. Rutherford Backscattering Spectrometry (RBS) was used for absolute Zr, Si and Ar quantification using $^4He^{2+}$ or $^4He^+$ beams with energies from 1.0 to 3.0 MeV with a surface barrier detector set at 165°. The absolute amount of carbon and oxygen was determined by Nuclear Reaction Analysis (NRA) using $^{16}O(d,p_1)^{17}O$ and $^{12}C(d,p)^{13}C$, with energies 890 and 980 keV respectively, with the surface barrier detector set at 150°. For the H quantification we used Elastic Recoil Detection Analysis (ERDA) using a 3.0 MeV $^4He^{2+}$ beam, with the surface barrier detector set at 35° and a 13-μm Mylar filter to stop the scattered alpha particles.

Fourier Transform Infrared (FTIR) spectra were collected in transmission at normal geometry under dry nitrogen atmosphere in a Nicolet 510 spectrometer. The microstructure of the films was examined by Scanning Electron Microscopy (Hitachi FESEM S-5200) for specimen deposited on the silicon wafer substrates.

Optical characterization was performed by reflectance measurements in the 400–1000 nm range. A Fourier Transform microspectrometer Bruker IF66/S was used.

The static permittivity of the films was obtained from measurements of capacitance at 100 kHz using a ESI2150-LCR apparatus The electrical contacts were made of Al evaporated at 10^{-1} Pa over a mask with 0.19 mm^2 area holes.

3. Results

3.1. Microstructure and chemical composition

The mixed Zr–Si oxide thin films were flat as previously observed by AFM and SEM images for the single oxides [10–12]. Standard diffraction Bragg–Brentano measurements did not show any defined structure in the films. In addition, the samples were featureless in cross-sectional SEM analysis.

Fig. 1 shows the correlation between the partial pressure ratio between the TrEOS and ZTB volatile precursors and the relative atomic concentration (i.e., x in $Zr_xSi_{1-x}O_2$) in the films determined by RBS. Note that for the same partial pressure of Si and Zr precursors, the films are enriched in Zr content. This is consistent with a higher deposition rate observed for ZrO_2 with respect to SiO_2 for similar experimental conditions.

XPS analysis indicated the presence of C, O, Si, and Zr atoms at the sample surfaces. This C signal diminish to levels below ~5% after sputter cleaning with 400 eV O_2^+ ions during few minutes (sputtered thickness of 1–2 nm). Binding energies of Si 2p and Zr 3d photoelectron peaks and modified Auger

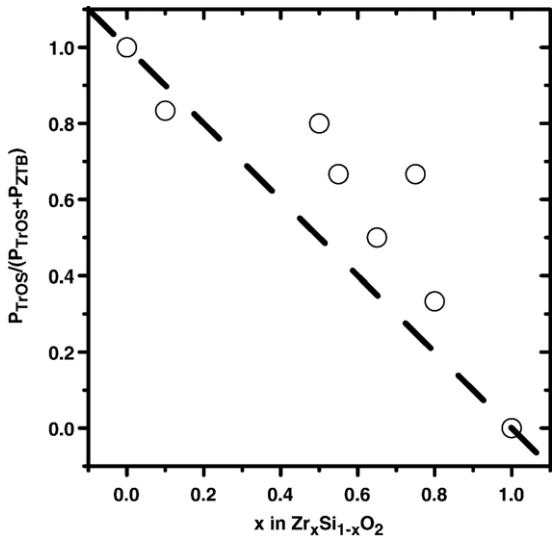

Fig. 1. Correlation between the relative partial pressures of the TrEOS and ZTB precursors and the composition x in $Zr_xSi_{1-x}O_2$ thin films prepared by IBICVD (see text).

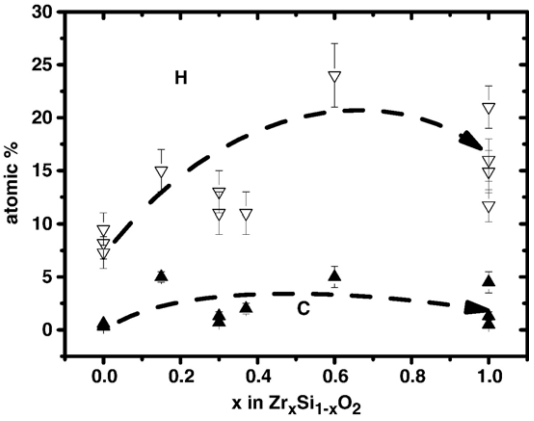

Fig. 2. H and C content as a function of the Si/Zr ratio for mixed oxides $Zr_xSi_{1-x}O_2$ ($0<x<1$) thin films prepared by IBICVD (see text).

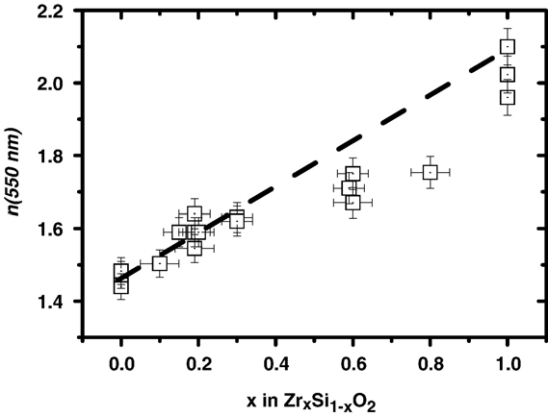

Fig. 4. Optical refractive index evaluated at 550 nm of $Zr_xSi_{1-x}O_2$ ($0<x<1$) thin films prepared by IBICVD.

parameters for SiO_2 and ZrO_2 thin films were consistent with reported values for these single oxide materials [17]. In the case of mixed oxides, an increase of the modified Auger parameter of both Si and Zr atoms for increasing relative Zr content in the films is observed (not shown).

Fig. 2 shows the content of H and C contaminants in the mixed oxide $Zr_xSi_{1-x}O_2$ ($0<x<1$) thin films prepared by IBICVD as described in the experimental section. We observe that the percentage of C atoms increases by increasing relative Zr content in the films from about 1% for pure SiO_2 to 5% for pure ZrO_2. The percentage of H atoms incorporated in the films also increases with the relative Zr content, from about 10% atomic for pure SiO_2 to ~15% for pure ZrO_2, with a maximum (23%) for $x=0.6$. The relative oxygen concentration (i.e., [O]/([Zr]+[Si]) was about 2.1 for SiO_2 and 2.2 for ZrO_2 . For intermediate stoichiometries, the relative oxygen concentration may even rise to 2.3–2.4 as for $x=0.6$–0.8 (errorbars of 5–10%). Despite these large errorbars, we have found always an excess of oxygen in the samples. It is also worth mentioning that about 1–3 at.% of Ar is incorporated in the films, disregarding the Zr/Si stoichiometry.

Fig. 3 shows FT-IR characterization for several $Zr_xSi_{1-x}O_2$ films. SiO_2 films are characterized by the principal transverse-optical (TO) modes of the Si–O–Si group identified as a rocking mode (TO_1 at ~460 cm^{-1}), a bending mode (TO_2 at ~800 cm^{-1}), and the asymmetric stretching mode (TO_1 at ~1070 cm^{-1}), [10,11]. For pure ZrO_2 films a broad band appears between 300 and 500 cm^{-1}. This band is attributed to badly order cubic and/or tetragonal zirconia phase [12]. For the zirconium silicates, a new broad band appears at 800–1100 cm^{-1} that is due to the formation of Zr–O–Si bonds. Besides, a clear signal from carboxylic groups is present in the films containing Zr (the –OH contribution appears at 2600–3500 cm^{-1} , the C═O bond at 1700 cm^{-1} and C–O at 1300–1400 cm^{-1}). Note how the carboxylic contribution increases with the zirconium content in the films and how only a negligible –OH contribution is detected in the pure SiO_2 films. The presence of carboxylic groups is enhanced when mixed oxides are produced, i.e., when both precursors are dosed simultaneously in the reactor. Besides, they are minimised when the O_2/Ar partial pressure ratio in the bombarding gas is decreased.

3.2. Optical characterization

Fig. 4 shows the optical refractive index evaluated at a wavelength of 550 nm (i.e., *n(550 nm)*) of a series of $Zr_xSi_{1-x}O_2$

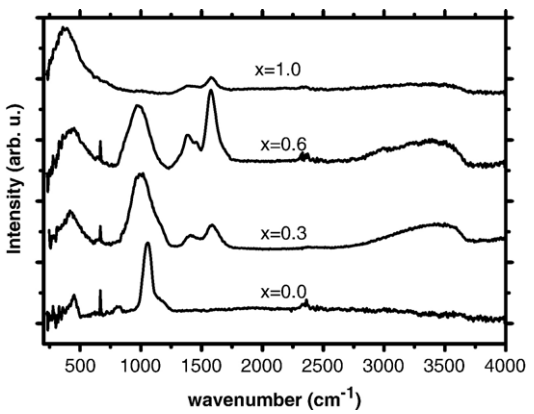

Fig. 3. FT-IR of several mixed oxide $Zr_xSi_{1-x}O_2$ thin films prepared by IBICVD (see text).

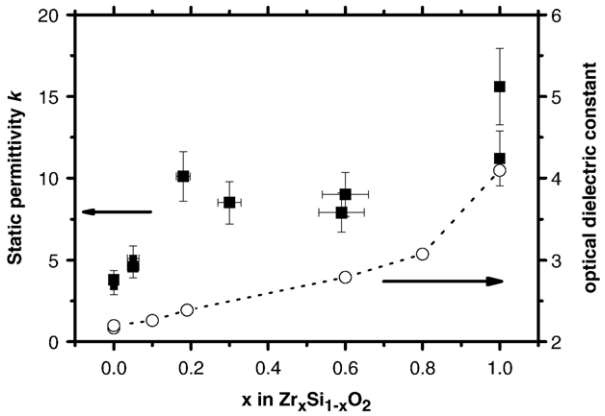

Fig. 5. Static permittivity and optical dielectric constant evaluated at 550 nm of $Zr_xSi_{1-x}O_2$ ($0<x<1$) thin films prepared by IBICVD.

($0<x<1$) thin films prepared by IBICVD with 400 eV with a mixture of O_2^+ and Ar^+ ions. We observe that *n(550 nm)* increases from 1.45 to 2.10 with the Zr content in the films. For zirconium silicates with $x<0.4$ and pure ZrO_2 ($x=1$), the values were close to those reported for compact materials, while for other stoichiometries ($0.6<x<0.8$) they were slightly below their linear interpolation.

3.3. Electrical characterization

The static permittivity k of $Zr_xSi_{1-x}O_2$ ($0<x<1$) thin films prepared by IBICVD using mixtures of O_2^+ and Ar^+ ions is represented in Fig. 5. It varies from ~4 for pure SiO_2 to 8–10 for $x=0.2$. Then, k remains approximately constant within the uncertainties of the measurements up to $x=0.6$. For higher Zr concentration in the films, k increases again to achieve values up to ~15 for pure ZrO_2. In this figure, the optical dielectric constant, obtained from the data in Fig. 4, is included for comparison. It is evident that the static and optical dielectric constants behave in a different manner.

4. Discussion

The $Zr_xSi_{1-x}O_2$ ($0<x<1$) thin films prepared by IBICVD with the conditions described in the experimental section are predominantly amorphous without phase segregation for intermediate Zr/Si compositions as deduced from FT-IR characterization. The presence of the new Zr–O–Si band, the strong diminishing of the Si–O–Si band in the spectra of intermediate stoichiometry zirconium silicates and the broad Zr–O–Zr band at 300–500 cm^{-1} support this idea [18]. Ballistic effects at the surface of the growing films as well as the incorporation of Ar atoms within the film for any Zr/Si composition contribute to increase the disorder during growth and therefore to the formation of amorphous structures. Although a systematic study of the stability of the films is not performed, note that the incorporated Ar in the Zr–O–Si network of the films is not released after thin film annealing at 300 °C for any x composition. Besides, it has been previously observed that the crystallization of ZrO_2 films prepared with Ar is strongly influenced by the presence of the Ar within the initial amorphous structure, and that this Ar does not disappear after heavy annealing at 800°C as reported in zirconium and iron oxides prepared with a similar methodology [12,19].

A significant amount of carboxylic groups is incorporated into the zirconium silicate thin films, as reported by the FT-IR characterization. Incorporation of carboxylates in the films is less favoured when Ar percentage in the bombardment gas is increased. Since the momentum transferred by 400 eV Ar^+ ions to the atoms at the film surface is more than twice that of 400 eV O_2^+ ions [20], a possible explanation for this effect might be that there is a threshold momentum that prevents the incorporation of these groups to the films. Another explanation might be the fact that the relative amount of atomic O^+ with respect to O_2^+ increase in a O_2/Ar plasma with respect to O_2 plasma alone [21]. This way the chemical reactivity of the bombarding gas would be increased, producing more complete oxidation of the ZTB precursor. Carboxylic groups are not reported in zirconia and zirconium silicates thin films prepared by thermal decomposition of the ZTB precursor [4,18], but the presence of C═O species is found in films prepared by the decomposition of ZTB by microwave plasma [14]. In fact, we have observed that the carboxylic groups are weakly linked to the film structure because they can be easily released after annealing at 300 °C.

In general low values of refractive index and permittivity for high zirconium containing silicates are justified by the presence of impurities in the form of hydroxyl and carboxylic groups in the films. Note for example that the refractive index of compact ZrO_2 thin films reported in the literature is 2.1 [22].

The smooth steady variation of the optical dielectric constant or refractive index with the Zr content in the films is justified by the reported variation of the polarizability between the ZrO_4 (low Zr content) and ZrO_8 units (high Zr content) present in the structure of amorphous zirconium silicates [3]. In practice, this represents a change from more covalent to more ionic bonding character as x is increased in $Zr_xSi_{1-x}O_2$ films. Note that the optical refractive index is linked to the microscopic polarizability through the Lorentz–Lorenz relation [3]. This justifies the variation of the optical refractive index with the stoichiometry of the films.

The non-linear correlation observed between stoichiometry and permittivity for zirconium silicates with $x<0.5$ has been reported previously [2,23]. It has been related to the change in coordination of Zr^{4+} cations between 4 for $x<0.1$ to 8 for $x>0.5$ [4]. It is well established that the contribution of infrared active modes to the static permittivity k is proportional to the square of its transverse infrared effective charge e_T^* [4]. On the other hand, e_T^* is proportional to the bond order, that for Zr–O bond is defined as the ratio of number of valence electrons available from each Zr atom to the number of O-atoms nearest neighbours. In the case of amorphous Zr–Si–O system, bond order varies between 1 for Zr diluted in a SiO_2 matrix and 0.5 present in $ZrSiO_4$ and ZrO_2. This change of coordination in amorphous Zr silicates has been confirmed by EXAFS studies [4]. Changes in the ionic and polar contributions to the static permittivity are very sensitive to local order, and therefore, this would justify the different behaviour of the static permittivity and the optical dielectric constant with the stoichiometry of the films.

5. Conclusions

We have reported on $Zr_xSi_{1-x}O_2$ thin films prepared by IBICVD at room temperature using 400 eV ions from a RF Ar/O_2 discharge. The films were amorphous and flat. The content of H (10–23 at.%) and C (1–5 at.%) in the films increased with the amount of Zr in the films. An important contribution of the H and C impurities in the films was in the form of carboxylic and hydroxyl groups. A 1–3 at.% of Ar atoms is incorporated in the films disregarding the Zr/Si content. No phase segregation of the pure single oxides is observed.

The refractive index at 550 nm of the films increases from 1.45 to 2.10 with the Zr content in the films. For zirconium silicates with $x<0.4$ and pure ZrO_2 ($x=1$), the values were close to those

reported for compact materials, while for other stoichiometries ($0.6<x<0.8$) they were slightly below their linear interpolation. In the case of the permittivity measurements in the static limit, a rapid increase of the permittivity for small amount of Zr in the films ($x<0.2$) is justified by the change in coordination of the Zr ions when diluted in a SiO_2 matrix, in agreement to a previously reported model [4].

Acknowledgments

We thank the Spanish Ministry of Science and Education for financial support (grant no. MAT 2004-01558).

References

[1] A. Feldman, E.N. Farbaugh, W.K. Haller, J. Vac. Sci. Technol., A, Vac. Surf. Films 4 (1986) 2969.
[2] G.D. Wilk, R.M. Wallace, Appl. Phys. Lett. 76 (2000) 112.
[3] G.M. Rignanese, F. Detraux, X. Gonze, A. Bongiorno, A. Pasquarello, Phys. Rev. Lett. 89 (2002) 117601.
[4] G. Lucovsky, G.B. Rayner Jr., Appl. Phys. Lett. 77 (2000) 2912.
[5] A.R. González-Elipe, F. Yubero, J.M. Sanz, Low Energy Ion Assisted Film Growth, Imperial College Press, 2003, p. 58.
[6] A.R. González-Elipe, J.P. Espinós, A. Barranco, F. Yubero, A. Caballero, J. Phys., IV 9 (1999) 699.
[7] F. Yubero, A. Stabel, A.R. González-Elipe, J. Vac. Sci. Technol., A, Vac. Surf. Films 16 (1998) 3477.
[8] A. Stabel, A. Caballero, J.P. Espinós, F. Yubero, A. Justo, A.R. González-Elipe, Surf. Coat. Technol. 100–101 (1998) 142.
[9] F. Gracia, F. Yubero, J.P. Holgado, J.P. Espinós, A.R. González-Elipe, T. Girardeau, Thin Solid Films 500 (2006) 19.
[10] A. Barranco, F. Yubero, J. Cotrino, J.P. Espinós, J. Benítez, T.C. Rojas, J. Allain, T. Girardeau, J.P. Riviere, A.R. González-Elipe, Thin Solid Films 396 (2001) 9.
[11] A. Barranco, F. Yubero, J.P. Espinós, J. Benítez, A.R. González-Elipe, J. Cotrino, J. Allain, T. Girardeau, J.P. Riviere, Surf. Coat. Technol. 142–144 (2001) 856.
[12] J.P. Holgado, J.P. Espinós, F. Yubero, A. Justo, M. Ocaña, J. Benítez, A.R. González-Elipe, Thin Solid Films 389 (2001) 34.
[13] W. Kim, S. Kang, S. Rhee, J. Vac. Sci. Technol., A, Vac. Surf. Films 21 (2003) L16.
[14] B. Cho, S. Lao, L. Sha, J.P. Chang, J. Vac. Sci. Technol., A, Vac. Surf. Films 19 (2001) 2751.
[15] V. Drinek, Z. Bastl, J. Subrt, J. Pola, Appl. Surf. Sci. 108 (1997) 203.
[16] J. García-López, F.J. Ager, M. Barbadillo Rank, F.J. Madrigal, M.A. Ontalba, A. Respaldiza, M.D. Ynsa, Nucl. Instrum. Methods Phys. Res., B Beam Interact. Mater. Atoms 161–163 (2000) 1137.
[17] M. Klasson, A. Berndtsson, J. Hedman, R. Nilsson, R. Nyholm, C. Nordling, J. Electron Spectrosc. Relat. Phenom. 3 (1974) 427.
[18] G. Lucovsky, G.B. Rayner, D. Kang, C.L. Hinkle, J.G. Hong, Appl. Surf. Sci. 234 (2004) 429.
[19] F. Yubero, M. Ocaña, A. Caballero, A.R. González-Elipe, Acta Mater. 48 (2000) 4555.
[20] M. Alvisi, S. Scaglione, S. Martelli, A. Rizzo, L. Vasanelli, Thin Solid Films 354 (1999) 19.
[21] A. Yanguas-Gil, J. Cotrino, A.R. González-Elipe, J. Phys., D, Appl. Phys. 40 (2007) 3411.
[22] S. Venkataraj, O. Kappertz, H. Weis, R. Drese, R. Jayavel, M. Luttig, J. Appl. Phys. 92 (2004) 3599.
[23] G.D. Wilk, R.M. Wallace, J.M. Anthony, J. Appl. Phys. 87 (2000) 484.